Computational catalysis

Defining the optimal inductive and steric requirements for a cross-coupling catalyst using the energetic span model☆

Sebastian Kozuch*, Sason Shaik

Institute of Chemistry and the Lise Meitner-Minerva Center for Computational Quantum Chemistry, Hebrew University of Jerusalem, Givat Ram Campus, 91904 Jerusalem, Israel

ARTICLE INFO

ABSTRACT

This paper interrogates the efficiency of a model cross-coupling reaction catalyzed by palladium complexes, using a quantum mechanical/molecular mechanical (QM/MM) methodology that permits 'independent' treatments of the inductive and steric effects of the phosphine ligands of the palladium catalysts. To test the efficiency of the catalyst we calculate turnover frequencies (TOFs), based on 'the energetic-span model' which considers the TOF determining transition state (TDTS) and TOF determining intermediate (TDI) as the reaction-rate controlling factors. Four different TDTS and TDI species are considered: the square planar diphosphine palladium complex, the anionic monophosphine, the T-shaped monophosphine, and the anionic phosphine-free species. Two different requirements are found to typify the most efficient catalysts: either bulky ligands that hinder the stabilization of diphosphines, or medium size ligands with high electron withdrawing power. Both conditions reduce the energetic span of the cycle by destabilizing the TDI more than the TDTS, thereby leading to enhanced TOFs. The approach used here can serve for future theoretical or experimental designs of new palladium catalysis.

© 2010 Elsevier B.V. All rights reserved.

1. Introduction

1.1. Cross-coupling

Cross-coupling reactions catalyzed by transition metal complexes have revolutionized the way chemists create new carbon–carbon bonds [1–9]. The main factors that affect the efficiency of a given ligand in the corresponding catalytic cycles seem to be its steric bulk and inductive properties [1–3,10–13]. The size of the ligand, traditionally measured as the cone (or Tolman's) angle [10,12–15], applies steric hindrance to the approach of different species to the metal center. In the case of phosphines, probably the most highly used ligands, the labile Pd–L bond affords a range of possible reaction pathways based on the palladium coordination number (monophosphine, diphosphine, etc.). These choice pathways are strongly dependent on the sheer bulk of the phosphine ligand. Thus, the bulk of the ligand determines whether or not the metal will have accessible coordination sites, and is the ori-

gin of monophosphine complexes generated by bulky phosphines. Accessible coordination sites improve the efficiency of the catalysts, while if these sites are occupied, as in the cases of high ligand concentrations, the catalyst is less efficient and the ligand is thought to "poison" the catalyst. Thus, for example, the PtBu$_3$ moiety was a key player in this line of bulky ligands, thoroughly analyzed in experimental [16–22] and theoretical [20,23–32] studies.

The second key factor that influences the catalytic efficiency is the electrostatic-inductive effect of the ligand, which gauges the charge on the metal center [10,12,13,33,34]. A highly electron withdrawing ligand (for instance PF$_3$) draws charge from Pd and facilitates reactions like the reductive elimination, and conversely it slows down the oxidative addition. By contrast, an electron releasing ligand like PtBu$_3$ creates the reverse effects [1–3,32] and induces conflicting tendencies of bulk vs. inductive effects. As a result, it is not easy to decide what factor is more decisive, and in fact, the common available guideline that electron rich phosphines are needed for efficient cross-coupling reactions [18,21] may reflect ligand bulk rather than electron richness of the Pd center. Consequently, it remains unclear how should one assess the interplay of steric and inductive effects in the design of a new catalyst.
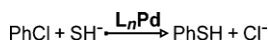
In this work we analyze an entire range of possible combinations of cone angles and inductive effects by independent assessments of their influences on the turnover frequency (TOF) of Pd catalysis. In reality, a ligand has both a specific cone angle and an inductive capability, and it is desirable to propose a theoretical treatment that can disentangle these properties. To this end, we used a hybrid

---

PhCl + SH⁻ →[**L_nPd**] PhSH + Cl⁻

Scheme 1. A model cross-coupling reaction used in this work.

quantum mechanical/molecular mechanical (QM/MM) approach, where the QM part permits the tuning of the inductive effect without affecting the cone angle, while the MM part is designed to provide the steric environment without affecting the electronic properties. With this methodology we could begin to determine the ligand characteristics that will provide the best cross-coupling catalyst.

1.2. The energetic span model

The efficacy of the cycle, i.e. its TOF, is a global rate function of all the states of the catalytic cycle. A development of a new catalyst with a single improved step (lower activation energy) will not necessarily lead to a better catalyst. For instance, a faster oxidative addition in a cross-coupling catalytic cycle would usually be accompanied by a slower reductive elimination, and hence the TOF will not necessarily be affected by such a change. To analyze a catalytic cycle, one needs a global kinetic model such as the recently developed and applied *energetic span model* [35–37]. In a steady state regime and based on the transition state theory, the TOF of the cycle is given by Eq. (1) [35,36]:

$$\text{TOF} = \frac{k_B T}{h} \frac{e^{-\Delta G_r / RT} - 1}{\sum_{i,j=1}^{N} e^{(T_i - I_j - \delta G'_{i,j})/RT}} \qquad \delta G'_{i,j} = \begin{cases} \Delta G_{rx} & \text{if } i > j \\ 0 & \text{if } i \le j \end{cases} \qquad (1)$$

where T_i and I_j are, respectively, the free energies of the ith TS and jth intermediate, while ΔG_{rx} is the reaction energy difference (the reaction driving force) for the process being catalyzed. ΔG_{rx} depends only on the reactants and products and is independent of the catalyst.

Usually only one TS and one intermediate are relevant to the kinetics of the entire cycle (with degree of TOF control close to 1 [35]). These two states are called TOF determining transition state (TDTS) and TOF determining intermediate (TDI). Using these as the sole relevant states, Eq. (1) can be simplified to:

$$\text{TOF} = \frac{k_B T}{h} e^{-\delta E / RT} \qquad (2)$$

δE, called the *energetic span*, is the apparent activation energy of the cycle. It is defined by means of the TDTS and the TDI as:

$$\delta E = \begin{cases} T_{\text{TDTS}} - I_{\text{TDI}} & \text{if the TDTS comes after the TDI} \quad (a) \\ T_{\text{TDTS}} - I_{\text{TDI}} + \Delta G_{rx} & \text{if the TDTS comes before the TDI} \quad (b) \end{cases} \qquad (3)$$

Note that the energetic span has different expressions depending on whether the TDTS appears after the TDI (Eq. (3a)), where δE is just the difference between the energies of these states, or when the TDTS precedes the TDI (Eq. (3b)), wherein the reaction energy is added.

1.3. A model cross-coupling reaction

With the energetic span approximation in mind (Eqs. (2) and (3)), we can calculate the TOF of the cycle knowing only the TDTS and TDI. In other words, if we know which states are the TOF determining ones, we just need to calculate these two states and not the full catalytic cycle. All other states may be neglected since they do not affect the TOF. To investigate the ligand effect, we used the cross-coupling model reaction (Scheme 1) used in our previous studies [35–38].
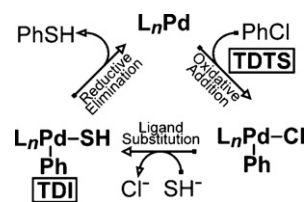
Scheme 2. A cross-coupling reaction cycle. The TDTS is the transition state for the oxidative addition step, while the TDI is the intermediate L_nPdPhSH [35–38].

The TDTS for the corresponding cycle was identified as the oxidative addition TS, and the TDI as the L_nPdPhSH complex (see Scheme 2) [35–38]. As such, these two states were used throughout this work to define the best catalyst for the model process, based on the above Eqs. (2) and (3).

The palladium catalyzed reaction can proceed by means of monophosphine or diphosphine-based mechanisms [11,23,24,26–29,31,32,38,39], it may prefer neutral or anionic species [21,25,38,40–44], and may even transpire by phosphine-free pathways [45–50]. Consequently, to find the best catalyst, we have to identify the one that has the smallest energetic span defined between the corresponding TDTS and TDI. The aim of this work is therefore to employ the energetic span model to search for the best catalyst of the model cross-coupling reaction (Schemes 1 and 2), using the cone angle and the inductive power of the phosphine ligands as independent variables.

2. Theoretical methods

The QM/MM approach was employed to achieve the separation of steric and inductive effects of the ligand on the reactivity of the catalyst, and at the same time avoid the artifacts that may arise due to a complete change in the nature of the ligand. A similar tactic has been applied previously (although using a different strategy) by Suresh and co-workers [51,52]. As a QM/MM approach we selected the ONIOM method implemented in Gaussian 03 [53]. The following strategy was used for separating steric and inductive effects:

2.1. Modulation of steric effects

The size of the ligand, measured as the cone angle [10], was gauged by generating a ring of 12 Ne atoms, treated with molecular mechanics. This technique resembles the He₈ model of Fey et al. [12,13,54]. By constraining distances and angles, the neon ring could be opened like an umbrella without altering the characteristics of the ligand, except obviously the cone angle (see Fig. 1). In the supplementary material we present examples of Gaussian 03 input files at several cone angles. The ligand (excluding the neon ring) has a fixed geometry and was calculated at a DFT level; therefore its QM features were completely independent from the cone angle.

We considered six cone angles, ranging from 118° to 218°; the smaller one is equivalent to the cone angle of PMe₃ (118°), while the largest one correspond to a ligand even bulkier than P(mesityl)₃ (212°) [10]. The Ne ring device provides a smoother steric repulsion profile compared with real ligands, and its cone angle is almost uniform throughout the circumference of the palladium center. However, in real systems and especially for phenyl-substituted phosphines, e.g. PPh₃ (145°), there are three "valleys" (areas of low effective cone angle between phenyls), and three "hills" (over the phenyls the effective cone angle is higher). The flexibility of real phosphines is also not accounted for by our cone angle device. Evidently the non-uniform cones and the flexibility of actual ligands provide a smaller effective cone angle that is not taken into account by the Ne ring model.
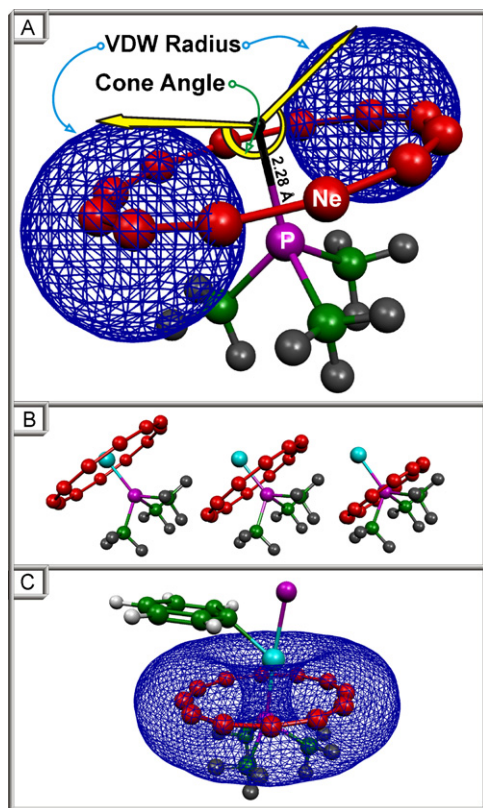
Fig. 1. (A) Definition of the cone angle [10,33]: the angle between the tangents of the Van der Waals spheres of the Ne atoms, with the vertex symmetrically located at 2.28 Å from the phosphorous. (B) Examples of the PdL fragments at cone angles of 138°, 178° and 218°. (C) An example of the steric hindrance caused by the Ne ring at 178° in the tri-coordinated Pd(L)PhCl complex. The blue toroid mesh depicts the inaccessible region generated in the UFF molecular mechanics model. At this high angle the tetra-coordinated Pd geometry is not possible. The cone angle modeled in this way does not affect the inductive effect of the ligand.

2.2. Modeling the inductive effect

To model the inductive effect, we considered the $P(CF_3)_3$ ligand in the QM part. The inductive power of this ligand can be gently modulated by altering the C–F distances while constraining the rest of the geometric parameters of the ligand. Whereas this procedure may be considered problematic since the geometry of each structure is not fully optimal, still the merit of the design outweighs this drawback. This approach enables to mimic the full range of possible electron withdrawing strengths: from the electron rich PtBu$_3$ all the way to the electron deficient PF$_3$. Furthermore, the C–F distance parameter changes the HOMO energy of a PdP$(CF_3)_3$ complex in a linear fashion. The HOMO is a gauge of the reactivity of the complex, and our calculations show a linear variation of the oxidative addition barriers as a function of the HOMO energies of the monophosphine palladium species. This relationship was tested using a model reaction (PdL + MeCl → PdLMeCl) where we changed the ligand, while computing both the oxidative addition and the HOMO energy of PdL. As can be seen in Fig. 2 [55], the variation is nicely linear. We considered five levels of the inductive effect, ranging from PdL having a HOMO energy at −0.157 hartree (C–F distance of 0.75 Å creates equivalence to PtBu$_3$) to −0.244 hartree (1.19 Å, equivalent to PF$_3$). This range covers, to the best of our experience, all the accessible electrostatic characteristics of real ligands. As such, the modifications of the $P(CF_3)_3$ model ligand behave like a series of real ligands differing in their inductive powers. Furthermore, changing the C–F distance in the $P(CF_3)_3$ ligand-series
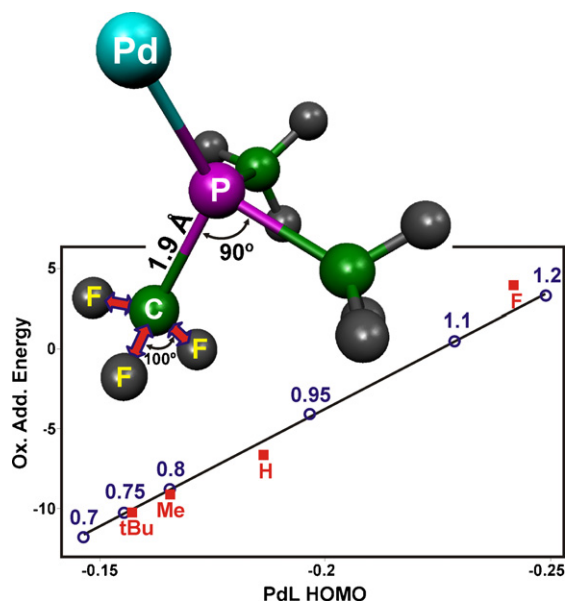
Fig. 2. Reaction energy of the oxidative addition of MeCl plotted vs. the HOMO level of the PdL complex. In filled squares, values for real PR$_3$ ligands. In empty circles, values for the modified $P(CF_3)_3$ "series of ligands", generated by varying the C–F bond distances (from 0.7 to 1.2 Å) while maintaining the rest of the ligand geometry fixed.

accounts nicely for the inductive effect without altering the cone angle.

2.3. QM/MM level

QM(DFT) calculations where carried out at the B3LYP level. The chosen basis set was lanl2dz augmented with an extra polarization function for C, P, Cl and S atoms [56]. The MM model used for the Ne ring was the universal force field (UFF) [57]. Only the QM energy was used for further analysis, as the MM part of the energy presents undesirable artifacts in strongly stretched systems. The Ne ring device can be viewed then as a phantom volume sterically forcing the QM section of the system, as can be seen in Fig. 1C, while the relative energy changes of the reaction species is given by the QM(B3LYP) part of the QM/MM energy. All the calculations where generated with the ONIOM method implemented in Gaussian03 [53].

As several of the species used are charged, the use of a solvent model was critical. ONIOM does not permit application of a continuum solvation model, so a QM single point with a solvent model, but obviously without the Ne ring, was used to estimate the solvation energy. The selected solvent was THF in the default IEF-PCM model defining the molecular cavity with the UAKS radii (an example of the input file is included in Supplementary material). Only the electrostatic term of the solvation energy was considered, as the non-electrostatic part was found to be of minor importance and in any event, it does not describe accurately the cavitation energy of these model ligands where the molecular volume is not well-defined.

2.4. Relative TOF calculation

In the reaction shown in Schemes 1 and 2 the TDI appears after the TDTS. Therefore, the energetic span of the cycle involves not only the energy difference of the two species, but also the reaction driving force ($\Delta G_{rx} = -21.6$ kcal/mol, independent of the catalyst,

Table 1
Relative TDTS energies for various steric/inductive combinations. Each cell contains, in parentheses, the label of the most accessible oxidative addition species,[a] and out of the parentheses its relative energy.[b].

HOMO[c]	Angle					
	118°	138°	158°	178°	198°	218°
−0.157	(4-N) −57	(4-N) −53	(4-A) −50	(3-A) −47	(3-A) −47	(3-A) −47
−0.179	(4-A) −52	(4-A) −51	(4-A) −49	(3-A) −47	(3-A) −47	(3-A) −47
−0.201	(4-A) −53	(4-A) −52	(4-A) −50	(3-A) −47	(3-A) −47	(3-A) −47
−0.223	(4-A) −56	(4-A) −55	(4-A) −51	(3-A) −47	(3-A) −47	(3-A) −47
−0.244	(4-A) −60	(4-A) −58	(4-A) −55	(3-A) −47	(3-A) −47	(3-A) −47

[a] Species: 4-N means neutral tetra-coordinated; 3-N, neutral tri-coordinated; 4-A, anionic tetra-coordinated; 3-A, anionic tri-coordinated.
[b] Energies in kcal/mol, relative to the energy of the fragments $Pd + 2L + PhCl + SH^-$.
[c] HOMO energies of the PdL complex in hartrees.

Table 2
Relative TDI energies for various steric/inductive combinations. Each cell contains the species label[a] of the lower energy intermediate (L_nPdPhSHCl complexes) and its relative energy.[b].

HOMO[c]	Angle					
	118°	138°	158°	178°	198°	218°
−0.157	(4-N) −104	(4-A) −97	(4-A) −87	(3-A) −82	(3-A) −82	(3-A) −82
−0.179	(4-A) −98	(4-A) −93	(4-A) −83	(3-A) −82	(3-A) −82	(3-A) −82
−0.201	(4-A) −95	(4-A) −91	(3-A) −82	(3-A) −82	(3-A) −82	(3-A) −82
−0.223	(4-A) −94	(4-A) −90	(3-A) −82	(3-A) −82	(3-A) −82	(3-A) −82
−0.244	(4-A) −95	(4-A) −90	(3-A) −82	(3-A) −82	(3-A) −82	(3-A) −82

[a] Species: 4-N, neutral tetra-coordinated; 3-N, neutral tri-coordinated; 4-A, anionic tetra-coordinated; 3-A, anionic tri-coordinated.
[b] Energies in kcal/mol, relative to the energy of the fragments $Pd + 2L + PhCl + SH^-$.
[c] HOMO energies of the PdL complex in hartrees.

see Eq. (3b)) according to Eq. (4b):

$$\text{TOF} \approx \frac{k_B T}{h} e^{-\delta E/RT} \tag{4a}$$

$$\delta E = T_{\text{TDTS}} - I_{\text{TDI}} - 21.6 \text{ kcal/mol} \tag{4b}$$

Having the apparent activation energy, we can calculate the TOF for each ligand. Clearly, the absolute values of these TOFs may have errors due to the limited accuracy of the B3LYP and QM(B3LYP)/MM methods. Even more, as small errors in the energetic span affect the TOF exponentially (Eq. (4a)), the absolute values of the TOF should be less accurate than the trends in the TOFs. Indeed, since we are interested in comparing ligand efficiency, all we need are the *relative* TOF values, which are much more accurate than absolute values, due to cancellation of errors.

3. Results

As discussed above, our modeling (Eqs. (2) and (3)) requires the energies of the TDTS and the TDI for a series of ligands. For the cross-coupling reaction depicted in Scheme 1, the oxidative addition is the TDTS and the L_nPdPhSH species is the TDI [35–38], where L can be a phosphine or a SH^-. But for each ligand type, these species can be different (being tri- or tetra-coordinated, anionic or neutral), as the characteristics of the complex may favor one coordination type over others. For instance, a phosphine with small cone angles can accommodate four ligands comfortably, and hence a Pd catalyst with small ligands will prefer a tetra-coordinated species route. However, when the phosphine has wider cone angles, the sterically demanding ligand will obstruct the respective high energy tetra-coordinated path, and the tri-coordinated complexes will become more accessible in spite of the incomplete saturation of the metal center.

In this study we tested four types of TSs and intermediates, which were considered as the most probable species in Pd cross-coupling pathways. These are the neutral or anionic, tetra- or tri-coordinated species, as can be seen in Fig. 3. The anionic mechanisms were examined since commonly the reaction medium contains small quantities of ions, which can form stable bonds to

the palladium [21,25,38,40–44]. The stability of these anionic complexes clearly depends on the nature [21,44] and concentration of the anions. In this work we considered the SH^- as the extrinsic anionic ligands (in addition to its role as the nucleophile); however the results may well vary when other charged species are present.
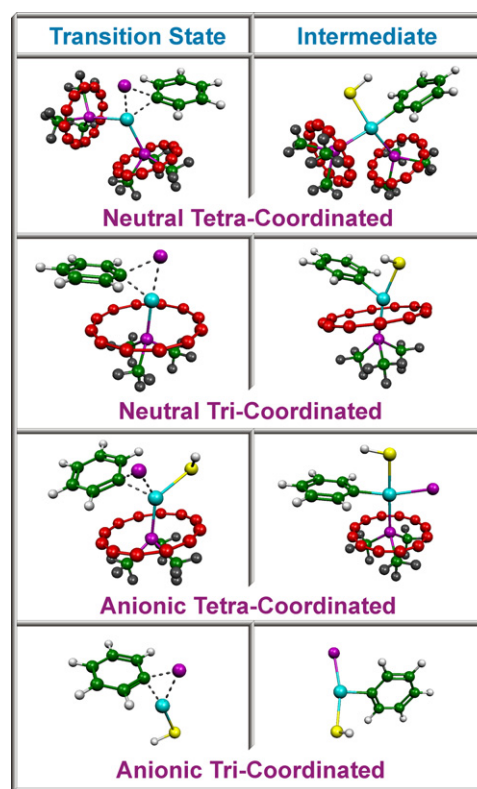
Fig. 3. Transition states and intermediates studied in this work. These are the TOF determining states (TDTS and TDI) of the different pathways. The energy difference of these species defines the energetic span (see Eqs. (2) and (3)).

Table 3
Energetic span (Eq. (4b))[a] for various steric/inductive combinations, specified by the cone angle/HOMO energy data.

HOMO[b]	Angle					
	118°	138°	158°	178°	198°	218°
−0.157	25	22	15	13	13	13
−0.179	24	20	12	13	13	13
−0.201	21	17	11	13	13	13
−0.223	17	13	9	13	13	13
−0.244	14	10	6	13	13	13

[a] At 25 °C in kcal/mol units.
[b] HOMO of the PdL complex in hartrees. The inductive effect increases down the columns.

Table 1 collects the features for the lowest energy TDTS of the four molecular species depicted in Fig. 3, while Table 2 gives the corresponding features for the TDI. The relative energies of these pairs of species define the energetic spans (Eq. (4b)), which are assembled in Table 3.

4. Discussion

The following observations can be made based on the data in Tables 1 and 2:

(a) As expected, bulkier phosphines hinder the bonding of other ligands.
(b) The diphosphine tetra-coordinated neutral TS or intermediate (4-N in Tables 1 and 2) can only be obtained in the case of the smallest cone angle and highest HOMO energy. This means that not only the size is important, but also the inductive effect, though to a lesser extent.
(c) At intermediate angles (138°, and most of 118° and 158° species) tetra-coordinated complexes are still preferred, but only in the anionic form (4-A in Tables 1 and 2). The thiolate anion is much smaller than phosphines, so it can snuggle easily in the coordination-sphere of the palladium to complete the ideal square planar type of complexes.
(d) With the bulkier ligands, the oxidative addition is so sterically impeded that only the highly energetic tri-coordinated anionic species could achieve the reaction (3-A in Tables 1 and 2). As can be seen in Table 3, the three highest cone angles possess phosphine-free species in the TDI and TDTS, thus the corresponding δE values are identical, resulting in an energetic span independent of the ligand structure. [50]
(e) No tri-coordinated neutral complexes (3-N) were found as lowest lying states. The SH⁻ ligand bonded to the metal has a comparable bond strength as the phosphine, but the size of the latter impedes the neutral tetra-coordinated molecules. If the cone angle gets higher than 158°, the T-shaped neutral tri-coordinated complexes become so unstable that the reaction can hardly occur, preferring full dissociation of phosphines. Again, we emphasize that this depends on the nature and concentration of anions, and on the solvent stabilization of charged species.
(f) As the cone angle grows, so does the energy of the two species (TDTS and TDI). Without a doubt bulky ligands lead to higher transition states. But, as we shall see, this does not necessarily mean a worse catalyst.

Let us first recall, what we explained in the introduction. Thus, since catalysis depends also on the TDI and on the sequence of appearance of the TDI and TDTS, a cycle with lower TDTS will not necessarily provide a better catalytic reaction [36,37]. The energetic span, as the apparent activation energy of the cycle, defines the catalytic efficiency: the smaller δE, the faster the reaction. Table 3 shows the energetic span calculated from the data in Tables 1 and 2, according to Eq. (4b). Table 4 shows the TOF according to Eq. (4a). It can be seen that bulky phosphines make good catalysts, in spite of their high energy TDTSs. The destabilization of the TDI runs almost parallel to the TDTS, so careful scrutiny of the energetic span is needed for assessing the efficiency.

In the particular reaction studied here, we found two basins of low energetic span: at high cone angle, and at moderate cone angle with high inductive factor. The fact that bulky phosphines provide active catalysts by obstructing the formation of diphosphines is widely recognized [16–32]. Our calculations clarify the root cause of this experimentally known trend. Thus, when bulky ligands prevent the formation of diphosphines complexes, the destabilization of the TDTS is lesser than that experienced by the TDI (Tables 1 and 2), thereby leading to a smaller δE (Table 3) and consequently higher TOF (Table 4).

To confirm this result, which originates from a model device for the cone angle, we compared the so obtained energetic spans to those obtained from full B3LYP calculations of "real" catalysts containing P*t*Bu₃ (cone angle of 182°) and PMe₃ (118°) (see details in Supplementary material). The resulting energetic spans for the "real" ligands were 14 and 28 kcal/mol, respectively, which are very close to the energetic spans of 13 and 25 kcal/mol obtained from the QM(B3LYP)/MM calculations of the modeled ligands, for the electron rich models with cone angles of 178° and 118° ($-0.157E_h$ in Table 3). It is clear from the energetic span model that the bulkier phosphine will generally form a cross-coupling catalyst with a TOF value several orders of magnitude faster than that of the smaller ligand PMe₃.

The fact that ligands with moderate cone angles and high inductive effects lead to efficient cross-coupling (with a maximum TOF at $-0.244E_h$ and 158° in Table 4) may appear as a surprise. Generally, electron rich ligands are thought to accelerate the oxidative addition step [18,21]. However, as explained above, the improvement of the oxidative addition step does not mean necessarily a more efficient catalytic cycle. The energetic span model shows that the energy of one transition state is only half of the story (Eqs. (2) and (3) [35–37,58]), since the electron rich phosphine will stabilize also the TDI, and as such, electron rich ligands will have at the most a minor effect on the overall catalysis. This conclusion is in accord with results by others [29].

Somewhat unexpectedly, our present results suggest that electron poor phosphines should be superior ligands for cross-coupling reactions. This success of electron deficient ligands was indeed observed recently for arylation reactions [59,60]. Electron withdrawing ligands generate smaller energetic span since they destabilize the TDI more than the TDTS. To verify this conclusion derived from the QM(B3LYP)/MM modeling we tested two real ligands, PMe₃ vs. P(CF₃)₃, by straightforward B3LYP calculations (see Supplementary material). The electron rich PMe₃ was found

Table 4
TOF (Eq. (4a))[a] for various steric/inductive combinations, specified by the cone angle/HOMO energy data.

HOMO[b]	Angle					
	118°	138°	158°	178°	198°	218°
−0.157	4×10^{-6}	4×10^{-4}	30	1000	1000	1000
−0.179	1×10^{-5}	7×10^{-3}	8000	1000	1000	1000
−0.201	4×10^{-3}	2	4×10^{4}	1000	1000	1000
−0.223	2	1000	1×10^{6}	1000	1000	1000
−0.244	700	5×10^{5}	2×10^{8}	1000	1000	1000

[a] TOF in s⁻¹ at 25 °C.
[b] HOMO of the PdL complex in hartrees. The inductive effect increases down the columns.

to have an energetic span of 28 kcal/mol, while the $P(CF_3)_3$ had only 15 kcal/mol, which are rather close to the QM(B3LYP)/MM results of 25 and 14 kcal/mol (for HOMO energies of −0.157 and −0.244 hartrees, at 118°). The outcome is quite clear: even though the fluorides generate a higher oxidative addition TDTS, it raises also the TDI such that the resulting energetic span becomes smaller and the corresponding catalyst is predicted to be more efficient.

All the above results confirm our general rule that *in catalysis there are no rate determining steps, but only rate determining states* [36,37]. The energetic span model projects this rule and provides a compact and useful model for understanding catalysis.

5. Conclusion

In this paper we studied the key states in the catalytic cycle of a model cross-coupling reaction catalyzed by palladium (Schemes 1 and 2) using a QM/MM methodology that permits independent treatments of the inductive and steric effects of the phosphine ligands of the catalyst. To test the efficiency of the various catalysts we used the energetic span model [35–37] which considers the TOF determining transition state (TDTS) and TOF determining intermediate (TDI) as the two states that control the rate of the cycle. Four pathways were considered to provide possible TDTSs and TDIs: the square planar diphosphine complex and anionic monophosphine, and the T-shaped monophosphine and anionic phosphine-free species.

The results show that when the cone angle of the phosphine is over 180°, and depending on the nature and concentration of the anions in the medium, the most stable species will be the tri-coordinated phosphine-free anionic complex. With moderate cone angles, the reaction will occur through the tetra-coordinated anionic monophosphine pathway. Only with small, electron rich phosphines like PMe_3 will the palladium catalyst prefer the textbook diphosphine mechanism (although this was found to be a rather inefficient mechanism).

Using the energetic span model we identified two factors that can increase the efficiency of cross-coupling palladium catalysts: A bulky ligand that hinders the stabilization of diphosphines, or a medium size ligand with high electron withdrawing power. Both conditions comply with the same requirements; the TDTS is less destabilized than the TDI, thus resulting in a small δE, and a large TOF.

It must be stated that the results obtained in this study are semi-quantitative, as the method used does not account for particular characteristics of specific phosphines, such as asymmetric or chelating ligands, its flexibility and mesomeric effects. Concentrations were not taken into account, and the study only included one kind of anionic ligand [44]. Additionally, a thiolate was used as the nucleophile for the reaction, which is rather uncommon, but was used for computational economy that enabled the many calculations done herein. Despite all these simplifications, the conclusions obtained in our study are physically correct and may serve as a guide for future theoretical or experimental research on design of catalysts.

Acknowledgments

Appendix A. Supplementary data

Examples of ONIOM input files, energies for the four TSs and Intermediates in gas phase and solvents, energies of the full QM calculations using $PtBu_3$, PMe_3 and $P(CF_3)_3$ as ligands, and CO vibrational frequencies of the $Ni(CO)_3L$ complex vs. HOMO of PdL can be found in the supplementary data associated with this article in the online version at doi:10.1016/j.molcata.2010.02.022.

References

[1] P. van Leeuwen, Homogeneous Catalysis, Understanding the Art, Kluwer Academic Publishers, Amsterdam, 2004.
[2] D. Astruc, Organometallic Chemistry and Catalysis, Springer-Verlag Berlin Heidelberg, 2007.
[3] R.H. Crabtree, The Organometallic Chemistry of the Transition Metals, 4th ed., Wiley-Interscience, New Jersey, 2005.
[4] S.L. Buchwald, Acc. Chem. Res. 41 (2008) 1439, and all the special issue on cross-coupling, Acc. Chem. Res. 41 (2008).
[5] K.C. Nicolaou, P.G. Bulger, D. Sarlah, Angew. Chem. Int. Ed. 44 (2005) 4442.
[6] N. Miyaura, A. Suzuki, Chem. Rev. 95 (1995) 2457.
[7] A. Jutand, Chem. Rev. 108 (2008) 2300.
[8] J.F. Hartwig, Acc. Chem. Res. 41 (2008) 1534.
[9] J.F. Hartwig, Nature 455 (2008) 314.
[10] C. Tolman, Chem. Rev. 77 (1977) 313.
[11] V.P. Ananikov, D.G. Musaev, K. Morokuma, Eur. J. Inorg. Chem. 34 (2007) 5390.
[12] N. Fey, Dalton Trans. 39 (2010) 296.
[13] N. Fey, A.G. Orpen, J.N. Harvey, Coord. Chem. Rev. 253 (2009) 704.
[14] D. White, N.J. Coville, Adv. Organomet. Chem. 36 (1994) 95.
[15] K.A. Bunten, L. Chen, A.L. Fernandez, A.J. Poe, Coord. Chem. Rev. 233–234 (2002) 41.
[16] R. Martin, S.L. Buchwald, Acc. Chem. Res. 41 (2008) 1461.
[17] R. Chinchilla, C. Nájera, Chem. Rev. 107 (2007) 874.
[18] U. Christmann, R. Vilar, Angew. Chem. Int. Ed. 44 (2005) 366.
[19] T.E. Barder, S.D. Walker, J.R. Martinelli, S.L. Buchwald, J. Am. Chem. Soc. 127 (2005) 4685.
[20] T.E. Barder, M.R. Biscoe, S.L. Buchwald, Organometallics 26 (2007) 2183.
[21] A. Littke, M. Soumeillant, R.F. Kaltenbach, R.J. Cherney, C.M. Tarby, S. Kiau, Org. Lett. 9 (2007) 1711.
[22] K.H. Shaughnessy, R.S. Booth, Org. Lett. 3 (2001) 2757.
[23] R. Álvarez, O. Nieto Faza, A.R. de Lera, D.J. Cárdenas, Adv. Synth. Catal. 349 (2007) 887.
[24] R. Álvarez, O. Nieto Faza, C. Silva López, A.R. de Lera, Org. Lett. 8 (2006) 35.
[25] L.J. Goossen, D. Koley, H.L. Hermann, W. Thiel, J. Am. Chem. Soc. 127 (2005) 11102.
[26] M. Ahlquist, P. Fristrup, D. Tanner, P. Norrby, Organometallics 25 (2006) 2066.
[27] M. Ahlquist, P. Norrby, Organometallics 26 (2007) 550.
[28] K.C. Lam, T.B. Marder, Z. Lin, Organometallics 26 (2007) 758.
[29] Z. Li, Y. Fu, Q. Guo, L. Liu, Organometallics 27 (2008) 4043.
[30] T. Barder, S.L. Buchwald, J. Am. Chem. Soc. 129 (2007) 12003.
[31] A.C. Braga, G. Ujaque, F. Maseras, Organometallics 25 (2006) 3647.
[32] T.R. Cundari, J. Deng, J. Phys. Org. Chem. 18 (2005) 417.
[33] C.A. Tolman, J. Am. Chem. Soc. 92 (1970) 2953.
[34] O. Kühl, Coord. Chem. Rev. 249 (2005) 693.
[35] S. Kozuch, S. Shaik, J. Am. Chem. Soc. 128 (2006) 3355.
[36] S. Kozuch, S. Shaik, J. Phys. Chem. A 112 (2008) 6032.
[37] S. Kozuch, S.E. Lee, S. Shaik, Organometallics 28 (2009) 1303.
[38] S. Kozuch, A. Jutand, C. Amatore, S. Shaik, Organometallics 24 (2005) 2319.
[39] H. Lakmini, I. Ciofini, A. Jutand, C. Amatore, C.J. Adamo, Phys. Chem. 112 (2008) 12896.
[40] S. Kozuch, S. Shaik, A. Jutand, C. Amatore, Chem. Eur. J. 10 (2004) 3072.
[41] P. Fristrup, M. Ahlquist, D. Tanner, P. Norrby, J. Phys. Chem. 112 (2008) 12862.
[42] L.J. Goossen, D. Koley, H.L. Hermann, W. Thiel, Organometallics 24 (2005) 2398.
[43] L.J. Goossen, D. Koley, H.L. Hermann, W. Thiel, Organometallics 25 (2006) 54.
[44] S. Shekhar, J.F. Hartwig, Organometallics 26 (2007) 340.
[45] M. Ahlquist, G. Fabrizi, S. Cacchi, P. Norrby, J. Am. Chem. Soc. 128 (2006) 12785.
[46] B. Xin, Y. Zhang, K. Cheng, J. Org. Chem. 71 (2006) 5725.
[47] X. Wang, D.V. Gribkov, D.J. Sames, Org. Chem. 72 (2007) 1476.
[48] C. Qin, W. Lu, J. Org. Chem. 73 (2008) 7424.
[49] S. Kang, H. Lee, S. Jang, T. Kim, S. Pyun, J. Org. Chem. 61 (1996) 2604.
[50] In a recent paper Carrow, Hartwig found active anionic phosphine-free complexes (which they called "ligandless") for the Heck reaction, originated from species containing the bulky PtBu3 ligand. See: B.P. Carrow, J.F. Hartwig, J. Am. Chem. Soc. 132 (2010) 79.
[51] J. Mathew, T. Thomas, C.H. Suresh, Inorg. Chem. 46 (2007) 10800.
[52] C.H. Suresh, Inorg. Chem. 45 (2006) 4982.
[53] M.J. Frisch, et al., Gaussian 03 (Revision C.02), Gaussian Inc., Wallingford, CT, 2004.
[54] N. Fey, A.C. Tsipis, S.E. Harris, J.N. Harvey, A.G. Orpen, R.A. Mansson, Chem. Eur. J. 12 (2006) 291.
[55] Traditionally the inductive effect is measured by considering the CO stretching frequency of the $Ni(CO)_3L$ complex [10,33,34]. Our calculations show an almost linear correspondence between this frequency and the HOMO of the PdL molecule (see Supplementary material). The HOMO level is easier to calculate and more accurate in theoretical chemistry, so it was the preferred variable to address for the inductive effect in this work.

[56] https://bse.pnl.gov/bse/portal. K.L. Schuchardt, B.T. Didier, T. Elsethagen, L. Sun, V. Gurumoorthi, J. Chase, J. Li, T.L. Windus, J. Chem. Inf. Model 47 (2007) 1045.

[57] A.K. Rappé, C.J. Casewit, Colwell, W.M. Goddard III, W.A. Skiff, J. Am. Chem. Soc. 114 (1992) 10024.

[58] C. Amatore, A. Jutand, J. Organomet. Chem. 576 (1999) 254.

[59] A.G. Sergeev, G.A. Artamkina, I.P. Beletskaya, Tetrahedron Lett. 44 (2003) 4719.

[60] J.D. Hicks, A.M. Hyde, A.M. Cuezva, S.L. Buchwald, J. Am. Chem. Soc. 131 (2009) 16720.